Fixed Points in Distance Recurrence Formulas

Federico Thomas

Abstract This paper shows how the position analysis of mechanisms with coupling number one can be solved by computing the fixed points of monotonic recurrent formulas. This new approach is directly elaborated on the 3-RPR planar mechanism.

Key words: Position analysis, spectahedra, fixed points, distance geometry.

1 Introduction

A myriad of papers have been written on the position analysis of serial and parallel robots. Roughly speaking, general methods can be divided into numerical or algebraic. While numerical methods directly compute these solutions from a set of closure equations, algebraic methods are concerned with the derivation of a resultant polynomial, of the lowest possible degree, from the mentioned closure equations whose roots determine the sought solutions. Thus, it is essential to chose the right closure conditions as they determine the complexity of the subsequent steps. Distance-based closure conditions have emerged as a good alternative to closure conditions based on kinematic loop equations. In this paper, we further investigate distance-based closure conditions by formulating them in terms of monotonic recurrences (self-maps). Then, the sought solutions are fixed points of these recurrences. Due to space limitations, these ideas are mostly visually presented for a particular example: the planar 3-RPR. Although they are applied to a particular example, it will be clear that no particularity of this mechanism is used at any time, except the fact that its coupling number is one. In other words, the presented approach can be directly applied to all mechanisms whose position analysis can be reduced to perform a kinematic inversion in a strip of tetrahedra (or triangles) [1].

Federico Thomas
Institut de Robòtica i Informàtica Industrial (CSIC-UPC), ETSEIB, Diagonal 647, Pavelló E, 08028 Barcelona, Spain. e-mail: f.thomas@csic.es

2 Computing unknown distances from known ones

The valid distances between a set of points depends on the dimension of the embedding space. These valid distances can be characterized using the so-called Cayley-Menger determinants [2]. The Cayley-Menger bi-determinant of two sets of points, $P_{i_1}, \ldots, P_{i_n}$ and $P_{j_1}, \ldots, P_{j_n}$, is defined as

$$\Pi\begin{pmatrix} i_1, \ldots, i_n \\ j_1, \ldots, j_n \end{pmatrix} \triangleq \begin{vmatrix} 0 & 1 & \ldots & 1 \\ 1 & s_{i_1,j_1} & \ldots & s_{i_1,j_n} \\ 1 & \vdots & \ddots & \vdots \\ 1 & s_{i_n,j_1} & \ldots & s_{i_n,j_n} \end{vmatrix}, \tag{1}$$

where $s_{i,j} = d_{i,j}^2 = \overline{P_i P_j}^2$. If the two sets of points in (1) coincide, the resulting determinant is said to be a Cayley-Menger determinant, which we will simply denote as $\Pi(i_1, \ldots, i_n)$.

In $\mathbb{R}^n$, any Cayley-Menger determinant involving more than n+1 different points vanishes. Therefore, given four points in $\mathbb{R}^2$, say P_i, P_j, P_k, and P_l, we have that

$$\Pi(i, j, k, l) = 0. \tag{2}$$

This equation permits expressing any pairwise distance between these four points as a function of the other pairwise distances. In particular, for $s_{k,l}$, we have that

$$s_{k,l}^{\pm}(i, j, k, l) = -\frac{1}{\Pi(i, j)} \left(\Pi\begin{pmatrix} i, j, k \\ i, j, l \end{pmatrix}\Big|_{s_{k,l}=0} \pm \sqrt{\Pi(i, j, k)\, \Pi(i, j, l)} \right), \tag{3}$$

where the notation next to the right hand side of the bideterminant indicates that all instances of $s_{k,l} = s_{l,k}$ appearing in it must be set to zero. Due to the square root, we have two possible values for $s_{k,l}$ corresponding to the two possible locations of points P_k and P_l with respect to the line supporting $\overline{P_i P_j}$. In what follows, $s_{k,l}^{+}(i, j, k, l)$ and $s_{k,l}^{-}(i, j, k, l)$ will denote these two solutions.

3 Cayley spectrahedra

Let us consider four points in $\mathbb{R}^2$, say P_1, P_2, P_3, and P_4, where all except two pairwise distances between them are known. Then, two situations arise up to index permutations which are next analyzed in detail.

Consider the quadrilateral bar-and-joint framework in Fig. 1(left) where the numerical values next to each bar stand for its squared length. Since this framework is embedded in $\mathbb{R}^2$, the volume of the tetrahedron formed by the four joint centers vanishes. That is, $\Pi(1, 2, 3, 4) = 0$, which implicitly defines the curve in the plane of the unknown distances $(s_{1,3}, s_{2,4})$ (see Fig. 1(right)). In general, this curve has branches that do not correspond to valid distances of $s_{1,3}$ and $s_{2,4}$ because they do not

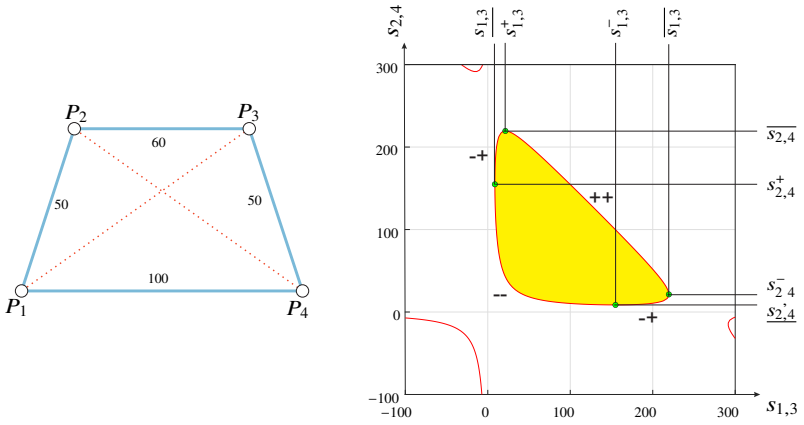

$$\Pi(1,2,3,4) = -2s_{1,3}^2 s_{2,4} - 2s_{1,3}s_{2,4}^2 + 520s_{1,3}s_{2,4} + 1000s_{1,3} + 1000s_{2,4} - 420000 = 0$$

Fig. 1 Bar-and-joint framework (left) and its associated spectrahedron shown in yellow (right) whose boundary corresponds to the valid lengths of the two dotted segments in the framework. Due to the convexity of spectrahedra, this boundary determines four monotonic one-to-one mappings between the lengths of the dotted segments in the framework.

satisfy the triangular inequalities. Only the boundaries of the oval region in yellow, technically known as a *Cayley spectrahedron* [3], correspond to valid distances. The orthotope tightly enclosing this spectrahedron can be easily computed as its bounds correspond to configurations in which the bar-and-joint framework has three aligned joints. According to the notation used in Fig. 1, it can be verified that these bounds are:

$$\begin{aligned}
\overline{s_{1,3}} &= \left[\min(d_{1,4} + d_{3,4}, d_{1,2} + d_{2,3})\right]^2 = 219.5445,\\
\underline{s_{1,3}} &= \left[\max(\mathrm{abs}(d_{1,2} - d_{2,3}), \mathrm{abs}(d_{1,4} - d_{3,4}))\right]^2 = 8.5786,\\
\overline{s_{2,4}} &= \left[\min(d_{1,4} + d_{1,2}, d_{3,4} + d_{2,3})\right]^2 = 219.5445,\\
\underline{s_{2,4}} &= \left[\max(\mathrm{abs}(d_{1,2} - d_{1,4}), \mathrm{abs}(d_{2,3} - d_{3,4}))\right]^2 = 8.5786.
\end{aligned}$$

Using expression (3), we can now express $s_{2,4}$ as $s^+_{2,4}(1,2,3,4)$ or $s^-_{2,4}(1,2,3,4)$ (that is, as a function of $s_{1,3}$). On the way round, we can express $s_{1,3}$ as $s^+_{1,3}(1,2,3,4)$ or $s^-_{1,3}(1,2,3,4)$ (that is, as a function of $s_{2,4}$). This allows us to subdivide the valid ranges for both $s_{1,3}$ and $s_{2,4}$, by computing the images of $\overline{s_{1,3}}$, $\underline{s_{1,3}}$, $\overline{s_{2,4}}$, and $\underline{s_{2,4}}$, , to end up with four one-to-one monotonic mappings between $\underline{s_{1,3}}$ and $s_{2,4}$. Each mapping will be identified using two signs, as shown in Fig. 1 (right).

Now, consider the bar-and-joint framework in Fig. 2 (left). In this case, the two variable distances share the point P_3. The corresponding spectahedron appears in Fig. 2 (right). This case is simpler than the previous one because the resulting

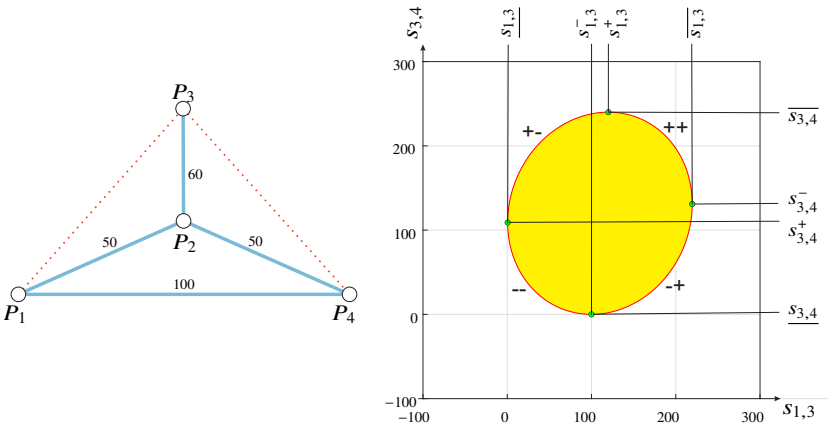

$$\Pi(1,2,3,4) = -120s_{1,3}^2 + 20s_{1,3}s_{3,4} + 24000s_{1,3} - 100s_{3,4}^2 + 21800s_{3,4} - 1200000 = 0$$

Fig. 2 Bar-and-joint framework (left) and its associated spectrahedron shown in yellow (right) whose boundary corresponds to the valid lengths of the two dotted segments in the framework. As in the case depicted in Fig. 1, this boundary determines four monotonic one-to-one mappings between the lengths of the dotted segments in the framework.

spectahedron is an ellipsoid [4] whose bounds are:

$$\overline{s_{1,3}} = \left(d_{1,2} + d_{2,3}\right)^2 = 219.5445, \qquad \overline{s_{3,4}} = \left(d_{2,4} + d_{2,3}\right)^2 = 219.5445,$$
$$\underline{s_{1,3}} = \left[\text{abs}(d_{1,2} - d_{2,3})\right]^2 = 0.4555, \qquad \underline{s_{3,4}} = \left[\text{abs}(d_{2,4} - d_{2,3})\right]^2 = 0.4555.$$

As in the previous case, we can subdivide the valid ranges for $s_{1,3}$ and $s_{3,4}$ to establish four one-to-one monotonic mappings between $s_{1,3}$ and $s_{2,4}$ which can be identified with two signs, as shown in Fig. 2 (right).

We have seen how the relationship between two pairwise distances defined by a set of four coplanar points can always be decomposed into four monotonic one-to-one mappings. This is the fundamental result on which relies the approach presented in this paper. It can actually be seen as a consequence of the convexity of spectrahedra (for an introductory account of spectrahedra, the reader is addressed to [5]).

4 Distance recurrences and their fixed points

Consider the 3-RPR planar robot in Fig. 3. It consists of a moving platform, defined by $\triangle P_4P_5P_5$, connected to a fixed base, defined by $\triangle P_1P_2P_3$, through the extensible legs defined by $\overline{P_1P_4}$, $\overline{P_2P_5}$, and $\overline{P_3P_6}$ [6].

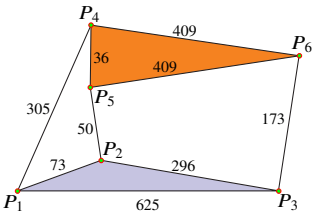

Fig. 3 Planar 3-RPR used as an example. The shown numerical values stand for the squared bar lengths.

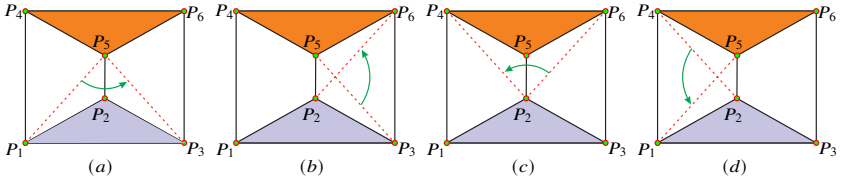

Fig. 4 A recurrence for $s_{1,5}$ of this 3-RPR planar robot can be obtained by expressing $s_{3,5}$ as a function of $s_{1,5}$ (a), $s_{2,6}$ as a function of $s_{3,5}$ (b), $s_{2,4}$ as a function of $s_{2,6}$ (c), and, finally, $s_{1,5}$ as a function of $s_{2,4}$.

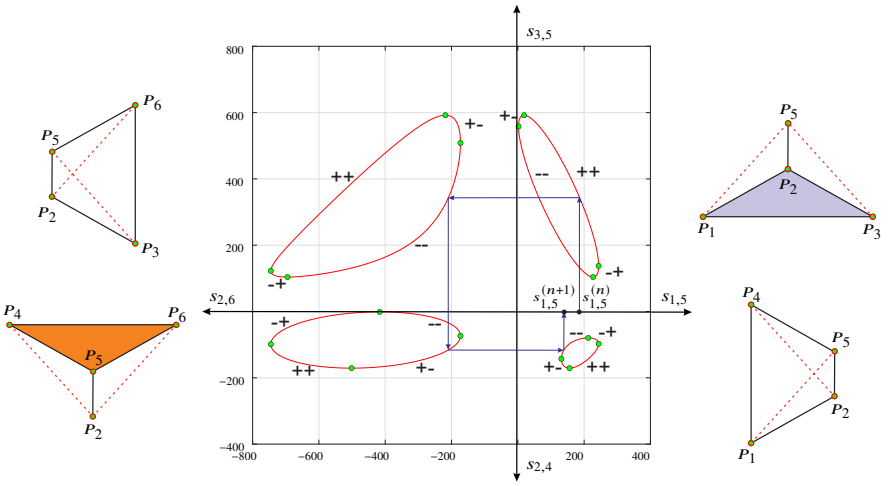

Fig. 5 There are 16 possible recurrences (self-mappings) for $s_{1,5}$, depending on the chosen set of signs identifying each monotonic branch of the spectahedra boundaries. Here we have applied the recurrence $(++, --, +-, --)$ to $s_{1,5}^{(n)}$ to obtain $s_{1,5}^{(n+1)}$.

A recurrence for $s_{1,5}$ of this planar robot can be obtained a follows: (1) since $\Pi(1,2,3,5) = 0$, we can express $s_{3,5}$ as a function of $s_{1,5}$; (2) since $\Pi(2,3,5,6) = 0$, we can likewise express $s_{2,6}$ as a function of $s_{3,5}$; (3) since $\Pi(2,4,5,6) = 0$, we can in turn express $s_{2,4}$ as a function of $s_{2,6}$; and (4), to complete the recurrence, we can express $s_{1,5}$ as a function of $s_{2,4}$ because $\Pi(1,2,4,6) = 0$ (see Fig. 4).

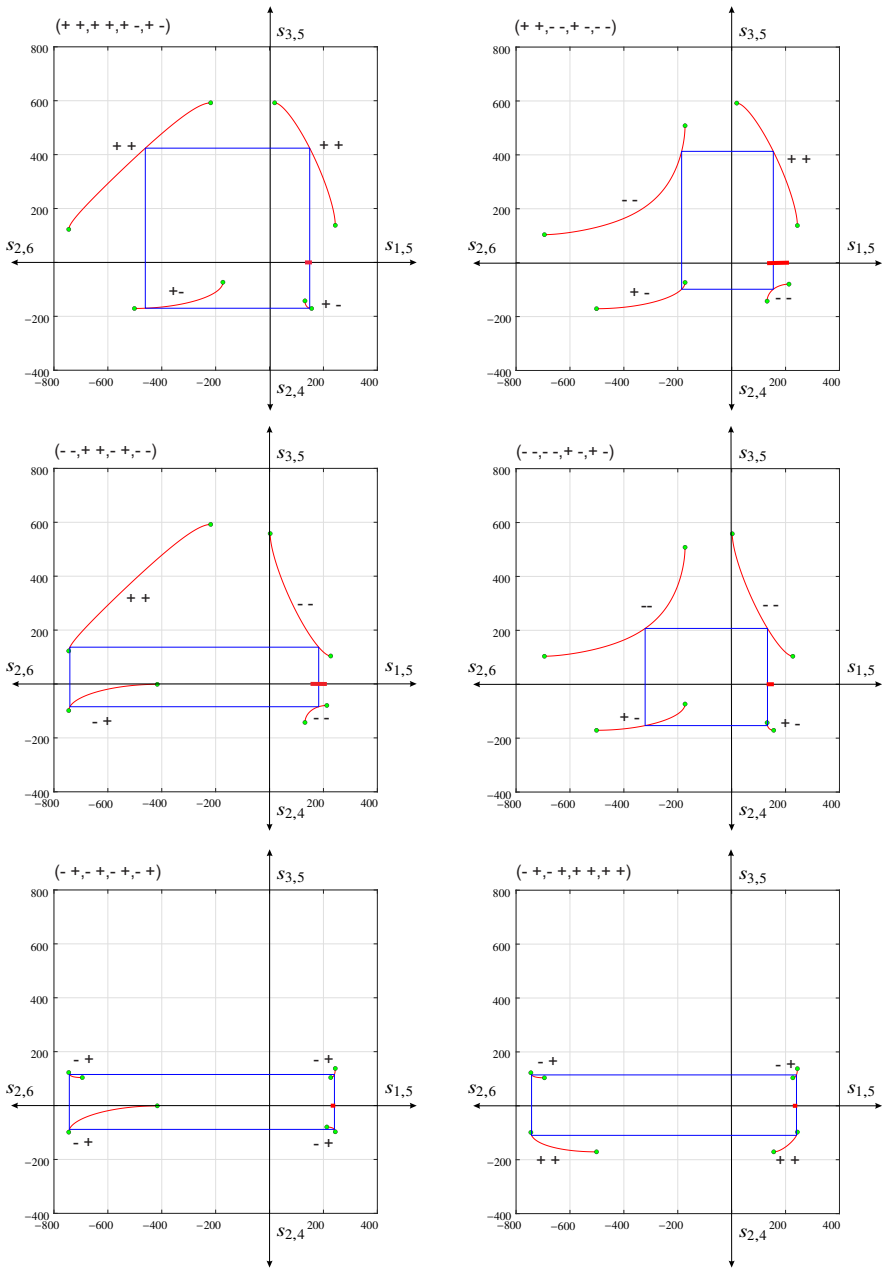

Fig. 6 Set of feasible recurrences. The valid interval domain for $s_{1,5}$ for each recurrence appears in red in its corresponding axis. The fixed points of these recurrences determine the parallelograms depicted in blue.

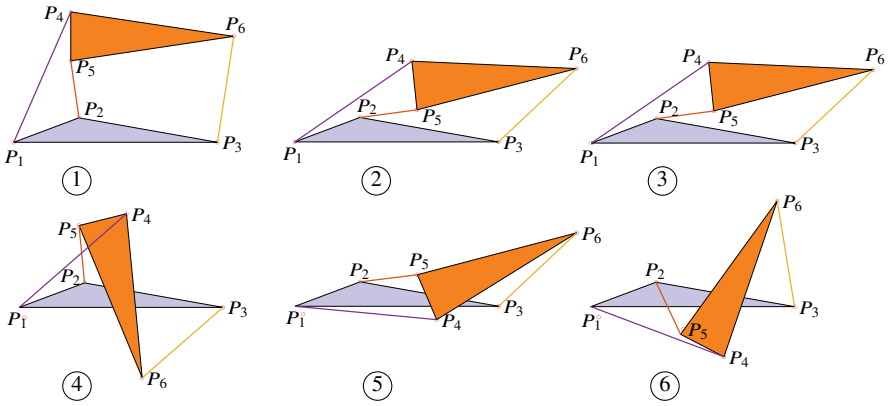

sol.	quadrant 1 branch	quadrant 2 branch	quadrant 3 branch	quadrant 4 branch	$s_{1,5}$	$s_{3,5}$	$s_{2,6}$	$s_{2,4}$
1	+ +	+ +	+ -	+ -	149.0000	424.0000	461.0000	170.0000
2	+ +	- -	+ -	- -	240.7641	115.3333	742.9421	88.4311
3	- -	+ +	- +	- -	182.3493	136.6145	740.9603	84.3431
4	- -	- -	+ -	+ -	154.4996	413.0476	185.6334	98.6403
5	- +	- +	- +	- +	240.5085	114.6584	742.4635	109.6414
6	- +	- +	+ +	+ +	132.8833	207.0809	321.0968	153.4463

Fig. 7 Solutions to the forward kinematics of the analyzed parallel mechanism obtained as fixed points of distance recurrences.

Using the values given in Fig. 3 for the known bar lengths, we can obtain the corresponding four spectrahedra which can be arranged on a plane divided into four quadrants, as shown in Fig. 5, so that the coordinate axes correspond to $s_{1,5}$, $s_{3,5}$, $s_{2,6}$, and $s_{2,4}$.

After decomposing the boundary of each spectrahedron into four monotonic branches, we can readily observe that the domain of one branch and the range of a previous branch in a given recurrence are, in some cases, disjoint. This implies that this recurrence is unfeasible. For example, the domain of $s_{1,5}$ for the $+-$ branch in the first quadrant and the range of $s_{1,5}$ for the $+-$ branch in the fourth quadrant are disjoint. This implies that all recurrences involving these two branches are unfeasible. To identify all unfeasible recurrences, we can propagate the initial domain for $s_{1,5}$, clockwise and/or counterclockwise, over all possible a priori recurrences. Then, if the result for a particular recurrence is the empty interval, we can conclude that it is unfeasible. This can be trivially implemented thanks to the monoticity of all branches. Fig. 6 shows the resulting six feasible recurrences and the domains of $s_{1,5}$ for each of them. Once we have identified the set of feasible recurrences and the domains for each variable, the problem consists in finding their fixed points. Nevertheless, they can be obtained by iterating the propagation of the valid intervals for $s_{1,5}$ over each recurrence. Indeed, let us take one of these recurrences and let

$\overline{s_{1,5}}$ denote the upper bound of the valid domain of $s_{1,5}$ for this recurrence. Let us also suppose that this upper bound is propagated counterclockwise. If the result is lower than $\overline{s_{1,5}}$, the recurrence is contractive at this point and the upper bound can be reduced accordingly. If the result is the same, we have identified a fixed point. If it is higher, the recurrence is expansive at this point, but this means that its inverse is contractive. As a consequence, this upper bound could also be reduced by changing the sense of the propagation. A similar reasoning can be applied to the lower bound. If this strategy is used in our example, we obtain the six fixed points given in Fig. 7. Observe that the relative orientation of $\triangle P_4P_5P_5$ with respect to that of $\triangle P_1P_2P_3$ is different in the first four solutions than in the other two. It can be proved that each recurrence determines the relative orientations for all the involved triangles. Therefore, we can choose beforehand those recurrences that lead to the desired orientations.

5 Conclusion

Given a planar rigid bar-and-joint framework with coupling number one, we have presented a way to derive monotonic distance recurrences and their variable domains so that their fixed points correspond to the valid framework configurations. We have used a particular mechanism to present some preliminary results using this new approach which obviously deserve a deeper mathematical analysis. Our current efforts concentrate on this latter point.

Acknowledgements This work has been partially supported by the Spanish National Plan for Scientific and Technical Research and Innovation through project PID2020-117509GB-I00/AEI/10.13039/50110001103).

References

1. Thomas, F., Porta, J.M.: Closure polynomials for strips of tetrahedra. In: J. Lenarcic, J.P. Merlet (eds.) Advances in Robot Kinematics 2016, vol. 4, pp. 303–312. Springer, Cham (2018)
2. Thomas, F., Porta, J.M.: Clifford's identity and generalized Cayley-Menger determinants. In: J. Lenarcic, B. Siciliano (eds.) Springer Proceedings in Advanced Robotics, vol 15. Springer, Cham (2021)
3. Sitharam, M., Gao, H.: Characterizing graphs with convex and connected Cayley configuration spaces. Discrete & Computational Geometry **43**(3), 594–625 (2010)
4. Thomas, F.: A distance geometry approach to the singularity analysis of 3R robots. Journal of Mechanisms and Robotics **8**(1), 011001 (2016)
5. Plaumann, D., Sturmfels, B., Vinzant, C.: Computing linear matrix representations of Helton-Vinnikov curves. In: H. Dym, M.C. De Oliveira, M. Putinar (eds.) Mathematical Methods in Systems, Optimization, and Control, pp. 259–277. Springer, Basel (2012)
6. Rojas, N., Thomas, F.: The forward kinematics of 3-RPR planar robots: A review and a distance-based formulation. IEEE Transactions on Robotics **27**(1), 143–150 (2011)